Helping cells jump to conclusions

Andreas Constantinou
Supervisor: Prof. Dr. Alejandro Colman-Lerner
University of Buenos Aires, Buenos Aires, Argentina
Supervisor: Prof. Dr. Miguel Teixeira
Instituto Superior Técnico, University of Lisbon, Lisbon, Portugal

October 28, 2014

Abstract

Many cellular processes rely on the ability of cells to sense and respond to chemical information in their immediate surroundings. Cells can achieve this by binding chemical signals (ligand) to specific receptor proteins, that convert the chemical information into intracellular signals to which the cells can respond. Furthermore, different concentrations of ligand may be distinguished by the fraction of bound to unbound receptor. Although this is generally only possible for concentrations that do not saturate the receptors, it was recently shown that cells' ability to distinguish between ligand concentrations could in theory be expanded into the saturating range, by the utilization of pre-equilibrium information resulting from the ligand–receptor binding kinetics. This mechanism was termed pre-equilibrium sensing and signaling (PrESS). Here, the possibility to biologically implement this idea as a simple, controllable genetic circuit is investigated. Via computational modeling and experiments it is shown that repression-based sensing, aided by slow influx of ligand, generates pre-equilibrium dynamics that may enable cells to distinguish between different saturating concentrations of ligand. Potential improvements are also discussed.

Keywords: binding kinetics, cell signaling, pre-equilibrium kinetics, systems biology

1 Introduction

Cells have evolved different strategies for sensing and responding to changes in their immediate surroundings. For example, through processes collectively known as signal transduction, cells can bind extracellular information in the form of signaling molecules (ligands) to ligand-specific receptors present in the plasma membrane. This binding converts the receptors from an inactive state into active signaling complexes, that then interact with signaling components inside the cell, thereby transmitting the extracellular information into the cell interior [1, 2].

The magnitude of the intracellular response is generally proportional to the fraction of receptors that are activated. As the extracellular concentration of ligand increases and more receptors get occupied by ligand, the intracellular response increases accordingly. However, this dependency is only possible while there are still free receptors available for binding ligand. When receptor occupancy is almost complete, increasing the ligand concentration even more will not significantly increase the fraction of bound receptors. Thus, based only on receptor occupancy levels cells would have all but no information for distinguishing between ligand concentrations that are saturating [1].

In a recent paper, Ventura and colleagues [3] proposed a mechanism that they termed pre-equilibrium sensing and signaling (PrESS), which they suggested may allow cells to shift their ability to distinguish between ligand concentrations into the saturating range. As the name suggests, PrESS takes advantage of differences in receptor occupancy levels before ligand binding reaches equilibrium. More specifically, through a combination of experiments and modeling, the authors showed that the rate at which a ligand–receptor binding reaction approaches equilibrium is inversely proportional to the concentration of ligand. As a result, although two saturating ligand concentrations may result in nearly indistinguishable fractions of ligand–receptor complex once the system reaches equilibrium, the amount of complex formed at a time point prior to equilibrium may still differ significantly. Thus, if downstream signaling from the receptor is fast enough to propagate binding information available in pre-equilibrium, cells could potentially differentiate between two saturating concentrations of ligand [3].

In addition, the authors also suggested that the response to pre-equilibrium information could be assisted by preventing signaling from occupied receptors once ligand binding has reached equilibrium. This would essentially extract only the pre-equilibrium information, while the uninformative equilibrium information would be muted. Through mathematical

modeling it was shown that such an effect could be achieved if the signaling response downstream of the activated receptors is transient [3].

While the idea underlying PrESS has been well characterized theoretically and mathematically, its biological relevance has yet to be demonstrated in practice. In this work, the potential for biologically implementing the idea of PrESS as a transcriptional network is investigated. Through a combination of theoretical modeling and experiments, an inducible genetic circuit capable of generating the dynamics necessary for PrESS is proposed.

2 Materials and methods

2.1 Strains and media

Yeast used for experimental circuit analysis were kindly provided by the original authors. In short, these strains were derivatives of the haploid yeast *Saccharomyces cerevisiae*. Yeast strain used for diffusion experiments was the W303a derivative ACL379 (genotype MATa, *leu*2-3,112, *trp*1-1, *can*1-100, *ura*3-1, *ade*2-1, *his*3-11,15, $\Delta bar1$) [4].

Yeast growth medium was a synthetic complete glucose-free medium with 2% galactose and 1% raffinose (SGR) (1.7 g/L yeast nitrogen base, 5 g/L ammonium sulfate, 0.79 g/L complete supplement mixture (MP Biomedicals), 2 mg/L adenine, 20 g/L D-galactose, 10 g/L D-raffinose).

2.2 Growth conditions

Circuit 1 and circuit2 steady state analyses were performed by inoculating circuit 1 or circuit 2 strains in 5 mL SGR medium and growing the cultures at 30°C with agitation until early exponential phase. Cultures were then diluted 100 times in 5 mL fresh SGR and induced with inducer from 100 times concentrated stock solutions in 100% ethanol or with a 100% ethanol control solution. Cells were then allowed to grow in the same conditions for 16 h more until low cell densities ($\sim 10^{-8}$ cells/mL). Cells were harvested and protein translation was blocked by adding the protein biosynthesis inhibitor cycloheximide [5, 6] to a final concentration of 25 μg/mL, from a 100 times concentration stock solution in 10% DMSO. Samples were kept at 4°C for 3 h to allow maturation of fluorescent proteins, after which cells were loaded in 384-well microplates for epifluorescence microscopy imaging. Samples were loaded in duplicate wells, yielding two technical replicates per sample.

Circuit 1 and circuit 2 time course analyses were performed by inoculating circuit 1 or circuit 2 strains in 5 mL SGR medium and growing the cultures at 30°C with agitation until early exponential phase. Cultures were diluted 100 times in 5 mL fresh SGR and allowed to continue growth until low cell densities ($\sim 10^{-8}$ cells/mL). Cultures were then again diluted 1:3 in 5 mL fresh SGR and cells allowed to adapt for 1 h before induction with inducer from 100 times concentrated stock solutions in 100% ethanol. Cultures were sampled at regular intervals over 9 h and protein translation was blocked with the protein biosynthesis inhibitor cycloheximide [5, 6] to a final concentration of 25 μg/ml. Samples were kept at 4°C for 15–24 h to allow maturation of fluorescent proteins, after which cells were loaded in 384-well microplates for epifluorescence microscopy imaging. Samples were loaded in duplicate wells, yielding two technical replicates per sample.

Inducer cell accumulation analysis was performed by inoculating ACL379 yeast in 5 mL SGR medium and growing the cultures at 30°C with agitation until early exponential phase. Cultures were diluted 100 times in 5 mL fresh SGR and allowed to continue growth until low cell densities ($\sim 10^{-8}$ cells/mL). Cultures were then again diluted 1:3 in 5 mL fresh SGR and cells allowed to adapt for 1 h before induction with inducer from 100 times concentrated stock solutions in 100% ethanol. Cultures were sampled at regular intervals over 5 h and immediately loaded in 384-well microplates for epifluorescence microscopy imaging. Samples were loaded in duplicate wells, yielding two technical replicates per sample.

2.3 Fluorescence microscopy

Yeast cell imaging was performed by epifluorescence microscopy using an Olympus IX81 microscope with an Olympus UPlanSApo 60x/1.35 oil immersion objective. Cells were illuminated with LEDs centered at 510 nm (FP1 and FP2) or 440 nm (inducer) through microscope excitation/emission filter cubes as shown in table 1, and emission was measured for either 300 ms (FP2 and inducer) or 500 ms (FP2). Imaging order was FP2, FP1, and inducer.

Fluorophore	Cube	Excitation	Dichroic	Emission
FP2	41004	HQ560/55x	Q595LP	HQ645/75m
FP1	41028	HQ500/20x	Q515LP	HQ535/30m
Inducer	31044v2	D436/20x	455DCLP	D480/40m

Table 1: Filter cubes used for fluorescence microscopy experiments.

2.4 Cell segmentation and quantification

Yeast cells were segmented and cell fluorescence was quantified using Cell-ID 1.4, an open-source software for segmentation and quantification of microscopy images of yeast cells [7]. In short, Cell-ID first segments cell boundaries based on out-of-focus brightfield images. Fluorescence images are then overlaid with their corresponding segmentation masks, allowing single-cell quantification of image intensities corresponding to cell fluorescence.

2.5 Fluorescence and statistical analysis

Cell fluorescence quantification data were imported from Cell-ID 1.4 to the statistical analysis software R 3.0.2 [8]. Background correction was carried out for all cells before statistical analysis by subtracting the background calculated by Cell-ID according to the formula:

$$F_{corr} = F_{tot} - A_{tot} \times F_{bg}, \quad (1)$$

where F_{corr} is the background corrected total cell fluorescence, F_{tot} is the original total cell fluorescence, A_{tot} is the total cell area in pixels, and F_{bg} is the mean background fluorescence per pixel calculated by Cell-ID.

Background corrected cell fluorescence data was used for all statistical analysis in R. Population fluorescence means and 99% confidence intervals were calculated by bootstrapping [9]. In short, each sample was resampled with replacement 4000 times, calculating the population mean after each round. The 4000 calculated means were then sorted in a vector from lowest to highest, and sample mean as well as lower and upper 99% confidence interval values selected by taking the mean values for vector positions 2000–2001, 20–21, and 3980–3981, respectively. Standard deviations were calculated with the innate function `sd()` in R.

2.6 Computational modeling

Computational modeling was performed in COPASI 4.11 (Build 65), a simulator for biochemical networks [10]. Mathematical models circuit1 and circuit 2 were adapted from the original study, and the model for studying the effect of slow inducer diffusion on X binding was derived from the circuit 1 and 2 models.

3 Results

As candidate circuits for generating the necessary dynamics for PrESS, two previously published transcriptional circuits, circuit 1 and circuit 2, were proposed.

The reasoning behind the use of circuits 1 and 2 for PrESS was that the binding reaction between X and Y should generate dynamics similar to those of ligand–receptor binding. If these dynamics could reflect onto the regulation of Z expression, this output should in principle be able to support PrESS.

Since binding between X and Y is a feature of both circuits, it was initially believed that X binding dynamics would be similar for both circuit 1 and 2. It was furthermore believed that the unique qualities of circuit 1 reported by the original authors could later benefit the downstream transient response. This led the analysis to initially focus on circuit 1.

3.1 X binding in circuit 1 is too fast to support PrESS

To investigate the potential of circuit 1 to generate the necessary pre-equilibrium dynamics, we wanted to study the dynamics of X binding upon exposure of the system to different concentrations of inducer. However, since we had no means of distinguishing between bound and unbound X, binding could not be observed experimentally.

To get at least a qualitative measure of the potential of the binding reaction to support PrESS, the pre-equilibrium dynamics of the system were studied computationally. For this analysis, the mathematical model developed by the original authors for circuit 1 (see original article) was adapted. This model, as well as that for circuit 2, had proven accurate in predicting the circuit's steady state dose-response behavior, and was therefore considered a good starting point also for the pre-equilibrium analysis.

By implementing the circuit 1 model in COPASI [10], dynamics of X binding upon induction were analyzed over time for different saturating levels of inputs. Although results indicated that the response time of X binding decreases with increasing levels of input, this effect was not reflected in the overall dynamics of Y synthesis (results not shown). These results were later verified experimentally with a yeast-implemented representation of circuit 1 (results not shown). Based on these results, it was concluded that the slow biochemical processes involved may limit the ability to propagate the upstream pre-equilibrium information from X binding.

3.2 Slow diffusion of inducer slows down inactivation

During the experimental analysis of circuit 1, it was observed that inducer accumulation in cells could be monitored by fluorescence microscopy. This revealed that inducer diffusion across the plasma membrane is remarkably slow, reaching equilibrium almost four hours after initial exposure (results not shown). Although this is not a new discovery, this unexpected finding significantly influenced the continuation of the analysis.

An important consequence of slow inducer diffusion is that the availability of inducer may become a limiting factor for the binding of Y to X. If the supply of Y to the reaction is much slower than the binding of Y to X, any inducer that diffuses into the cell will quickly be absorbed by unbound X molecules. This essentially makes X–Y binding directly proportional to the rate of ATc influx. Furthermore, since the influx of ATc is proportional to the extracellular concentration of the molecule [11], the rate at which inducer accumulates (and thereby the rate of the X–Y binding reaction) could be controlled via the concentration of inducer in the growth medium. If the concentrations selected are saturating, their distinct rates of diffusion will be reflected by the time it takes for X to be completely bound, and thereby the initiation of Z production. This is essentially a shift in response time where the time scale is defined by the diffusion rate constant rather than binding reaction rate constants (figure 1d).

For a given inducer concentration, the time until complete X binding is strongly dependent on the initial X levels in the cell. The more X present before induction, the more time will elapse before enough inducer has diffused into the cell to bind all X molecules. Consequently, since different concentrations of inducer give rise to different rates of X binding, larger initial pools of X will expand the difference in inactivation times between the inducer concentrations (figure 1d). This is an important difference compared to a non-diffusion limited binding reaction: since X is one of the reactants, increasing X concentrations will *decrease* the response time. In contrast, in the diffusion limited case, the increased reaction rate due to higher levels of X gets dominated by the slow supplementation of Y.

In circuit 1, the only low levels of X are available in the absence of inducer. Following the discussion above, it was believed that these levels may be too low for the system to take advantage of slow inducer diffusion. This could explain why no difference in reporter could be seen for different inducer concentra-

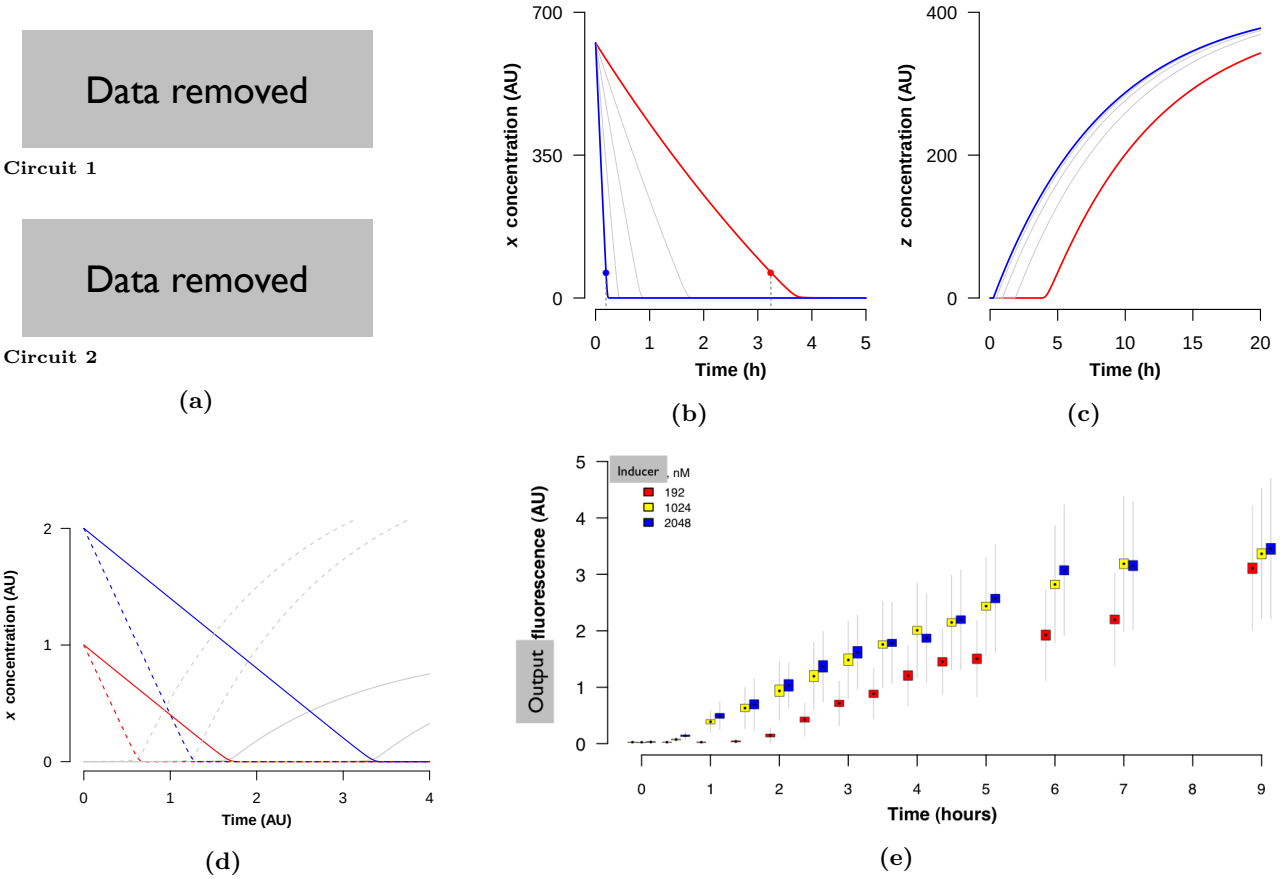

Figure 1: Circuit representations and results from circuit 2 analyses. (a) Visual representation of circuit 1 (top) and circuit 2 (bottom). X, Z, and Y represent X, Z, and Y, respectively. **(b)** Modeling results of X binding in circuit 2 for different saturating levels of inducer. Dots marking 90% inactivation indicate a shift in response times between high (blue line) and low (red line) inducer levels. **(c)** Modeling results of Z production in circuit 2 following the X binding in (b). Delayed initiation of production indicates that binding dynamics is reflected also in Z production. **(d)** Modeling results of X binding over time at two different saturating inducer concentrations. A higher concentration of inducer (dashed lines) binds X faster than a low concentration (unbroken lines), thus yielding a shift in response time. This shift expands with increasing X levels, since high initial levels of X (blue lines) take longer to bind than low (red lines). Gray lines show accumulation of *free* inducer. **(e)** Experimental results of Z production of circuit 2 yeast in response to different saturating inducer concentrations. At high concentrations of inducer (1024–2048 nM) Z production begins almost immediately, whereas a lower concentration (192 nM) delays the onset of expression with over an hour. Boxes span 99% confidence intervals and whiskers mark the standard deviation of each sample. Results from a single experiment, with sample sizes typically ranging between 100–1000 cells.

tions. However, it was hypothesized that the higher X levels in circuit 2 could be enough to support a diffusion-generated time response.

3.3 High basal X levels enables PrESS in circuit 2

To test the validity of this hypothesis, the computational analysis previously performed for circuit 1 was repeated for circuit 2. As before, the mathematical model developed by the original authors was adapted in COPASI. Furthermore, although this was not considered for the circuit 1 analysis, the diffusion of inducer was verified to correspond well with what had been observed experimentally by fluorescence microscopy. The model also indicated a more than 300-fold increase in pre-induction levels of X. This high increase in basal X levels was also observed experimentally in steady state experiments (results not shown).

In accordance to the previous computational analysis, X binding was studied over time in response to highly diverse but saturating levels of input. The results are presented in figure 1b and show that the high levels of X in the system prior to induction results in response times ranging from minutes to several hours. This is also reflected in the Z analysis, whose onset of expression is well timed with the complete binding of X (figure 1c). Importantly, the differences in Z concentrations between different levels of induction are larger earlier in the response, after which they progressively become smaller as expression levels approach steady state. This is precisely the behavior that is necessary for PrESS.

These modeling results were also verified experimentally with a yeast strain implementing circuit 2.

Z reporter production in response to a low-saturating inducer concentration (192 nM) was clearly differentiable from that of two higher saturating concentrations (1024 nM and 2048 nM) (figure 1e). This differentiation was the result of the 90-minute delay in the onset of Z production between the inputs.

These results indicate that X binding regulated by a slow-diffusing chemical inducer could potentially be a useful mechanism for generating the necessary dynamics for PrESS.

4 Discussion

An interesting observation from the circuit 2 analysis is that Z production does not start until nearly all X molecules have been bound by inducer. This can be seen in the results from the computational modeling, where the time point at which X is completely bound times well with Z production onset (figures 1b and 1c). It is also indirectly seen in the experimental results, where exposure to the low-saturating concentration of inducer leads to a 1.5 h delay during which no Z production is detected, followed by an almost instant switch to what appears to be the maximal production rate (figure 1e).

4.1 Different sensing may be a better choice for PrESS

The work presented here has given valuable insight on the use of a transcriptional network as a potential framework for synthetic implementation of PrESS. It has also highlighted several limiting factors that may complicate this implementation, in particular parameters that cannot easily be tuned and thereby set the experimental boundaries for the system.

However, it is important to note that successful implementation of PrESS does not only depend on shifting the response times, but also on the implementation of a downstream transient response. Such implementations will be intriguing challenges for the future.

References

[1] B. D. Gomperts, I. M. Kramer, and P. E. Tatham, *Signal Transduction*, 2nd ed. Academic Press, 22 September 2009, ch. 2, pp. 21–35.

[2] A. M. Stock, V. L. Robinson, and P. N. Goudreau, "Two-component signal transduction." *Annu Rev Biochem*, vol. 69, pp. 183–215, 2000.

[3] A. C. Ventura, A. Bush, G. Vasen, M. A. Goldín, B. Burkinshaw, N. Bhattacharjee, A. Folch, R. Brent, A. Chernomoretz, and A. Colman-Lerner, "Utilization of extracellular information before ligand-receptor binding reaches equilibrium expands and shifts the input dynamic range," *Proc Natl Acad Sci U S A*, vol. 111, no. 37, pp. E3860–9, Sep 2014.

[4] A. Colman-Lerner, A. Gordon, E. Serra, T. Chin, O. Resnekov, D. Endy, C. Gustavo Pesce, and R. Brent, "Regulated cell-to-cell variation in a cell-fate decision system," *Nature*, vol. 437, no. 7059, pp. 699–706, 09 2005. [Online]. Available: http://dx.doi.org/10.1038/nature03998

[5] T. G. Obrig, W. J. Culp, W. L. McKeehan, and B. Hardesty, "The mechanism by which cycloheximide and related glutarimide antibiotics inhibit peptide synthesis on reticulocyte ribosomes," *J Biol Chem*, vol. 246, no. 1, pp. 174–81, Jan 1971.

[6] T. Schneider-Poetsch, J. Ju, D. E. Eyler, Y. Dang, S. Bhat, W. C. Merrick, R. Green, B. Shen, and J. O. Liu, "Inhibition of eukaryotic translation elongation by cycloheximide and lactimidomycin," *Nat Chem Biol*, vol. 6, no. 3, pp. 209–217, 03 2010. [Online]. Available: http://dx.doi.org/10.1038/nchembio.304

[7] A. Bush, A. Chernomoretz, R. Yu, A. Gordon, and A. Colman-Lerner, "Using Cell-ID 1.4 with R for microscope-based cytometry," *Curr Protoc Mol Biol*, vol. Chapter 14, p. Unit 14.18, Oct 2012.

[8] R Core Team, *R: A language and environment for statistical computing*, R Foundation for Statistical Computing, Vienna, Austria, 2013. [Online]. Available: http://www.R-project.org/

[9] D. S. Fay and K. Gerow, "A biologist's guide to statistical thinking and analysis," *WormBook*, pp. 1–54, 2013.

[10] S. Hoops, S. Sahle, R. Gauges, C. Lee, J. Pahle, N. Simus, M. Singhal, L. Xu, P. Mendes, and U. Kummer, "COPASI—a COmplex PAthway SImulator," *Bioinformatics*, vol. 22, no. 24, pp. 3067–74, Dec 2006.

[11] H. C. Berg, *Random walks in biology*. Princeton University Press, 1993.